DIGITAL ACCESS TO SCHOLARSHIP AT HARVARD
DASH.HARVARD.EDU

HARVARD LIBRARY
Office for Scholarly Communication

Sequencing of Captive Target Transcripts Identifies the Network of Regulated Genes and Functions of Primate-Specific miR-522

Citation

Tan, Shen Mynn, Rory Kirchner, Jingmin Jin, Oliver Hofmann, Larry McReynolds, Winston Hide, and Judy Lieberman. 2014. "Sequencing of Captive Target Transcripts Identifies the Network of Regulated Genes and Functions of Primate-Specific miR-522." Cell Reports 8 (4) (August): 1225–1239. doi:10.1016/j.celrep.2014.07.023.

Published Version

doi:10.1016/j.celrep.2014.07.023

Permanent link

http://nrs.harvard.edu/urn-3:HUL.InstRepos:26869054

Terms of Use

This article was downloaded from Harvard University's DASH repository, and is made available under the terms and conditions applicable to Other Posted Material, as set forth at http://nrs.harvard.edu/urn-3:HUL.InstRepos:dash.current.terms-of-use#LAA

Share Your Story

The Harvard community has made this article openly available.
Please share how this access benefits you. Submit a story .

Accessibility

Cell Reports
Resource

OPEN ACCESS
CellPress

Sequencing of Captive Target Transcripts Identifies the Network of Regulated Genes and Functions of Primate-Specific miR-522

Shen Mynn Tan,[1,2] Rory Kirchner,[3] Jingmin Jin,[4] Oliver Hofmann,[3] Larry McReynolds,[4] Winston Hide,[3,5] and Judy Lieberman[1,2,*]
[1]Cellular and Molecular Medicine Program, Boston Children's Hospital, Boston, MA 02115, USA
[2]Department of Pediatrics, Harvard Medical School, Boston, MA 02115, USA
[3]Department of Biostatistics, Harvard School of Public Health, Boston, MA 02115, USA
[4]New England Biolabs, Ipswich, MA 01938, USA
[5]Harvard Stem Cell Institute, Cambridge, MA 02138, USA
*Correspondence: judy.lieberman@childrens.harvard.edu
http://dx.doi.org/10.1016/j.celrep.2014.07.023
This is an open access article under the CC BY-NC-ND license (http://creativecommons.org/licenses/by-nc-nd/3.0/).

SUMMARY

Identifying microRNA (miRNA)-regulated genes is key to understanding miRNA function. However, many miRNA recognition elements (MREs) do not follow canonical "seed" base-pairing rules, making identification of bona fide targets challenging. Here, we apply an unbiased sequencing-based systems approach to characterize miR-522, a member of the oncogenic primate-specific chromosome 19 miRNA cluster, highly expressed in poorly differentiated cancers. To identify miRNA targets, we sequenced full-length transcripts captured by a biotinylated miRNA mimic. Within these targets, mostly noncanonical MREs were identified by sequencing RNase-resistant fragments. miR-522 overexpression reduced mRNA, protein levels, and luciferase activity of >70% of a random list of candidate target genes and MREs. Bioinformatic analysis suggested that miR-522 regulates cell proliferation, detachment, migration, and epithelial-mesenchymal transition. miR-522 induces G1 cell-cycle arrest and causes cells to detach without anoikis, become invasive, and express mesenchymal genes. Thus, our method provides a simple but effective technique for identifying miRNA-regulated genes and biological function.

INTRODUCTION

Identification of microRNA (miRNA) target genes and the specific sequences they bind (miRNA recognition elements [MREs]) is important for understanding miRNA function (Bartel, 2009). Target prediction algorithms and experimental methods can be combined to identify candidate miRNA-regulated genes (Bartel, 2009; Thomas et al., 2010). However, even the best methods leave room for improvement. Target prediction algorithms are mostly based on a set of canonical rules for miRNA-mRNA interactions, in the 3′ UTR of the mRNA, mediated by complementarity to the seed region (nucleotides 2–8 of the miRNA). However, increasing evidence suggests that noncanonical MREs, involving bulges and G:U wobbles, pairing outside the seed and even "seedless" interactions, in the 3′ UTR as well as CDS, are not uncommon (Lal et al., 2009; Tay et al., 2008; Xia et al., 2012). The canonical rules may apply only to some miRNAs and to only a quarter of all miRNA-mRNA interactions overall (Helwak et al., 2013).

Biochemical isolation of target mRNAs bound to AGO and the RNA-induced silencing complex has improved MRE identification. AGO pull-down, combined with crosslinking and RNase digestion (high-throughput sequencing of RNA isolated by crosslinking immunoprecipitation [HITS-CLIP], crosslinking and immunoprecipitation followed by high-throughput sequencing [CLIP-Seq], and photoactivatable-ribonucleoside-enhanced crosslinking and immunoprecipitation [PAR-CLIP]), generates a global snapshot of miRNA-mRNA interactions (Chi et al., 2009; Hafner et al., 2010; Loeb et al., 2012; Zisoulis et al., 2010). However, these methods, even when combined with manipulation of miRNA expression, may not be adequate for identifying the mRNAs regulated by a particular miRNA. In fact, they usually rely on seed-based analysis or predictive algorithms to match the isolated MRE sequences to miRNAs. Recently, a novel unbiased method of mapping RNA-RNA interactions, termed crosslinking ligation and sequencing of hybrids (CLASH), was used to identify miRNA-MRE pairs by ligating bound MREs to their cognate miRNAs (Helwak et al., 2013). These global miRNA-binding methods are technically challenging, require large numbers of cells, and are most effective for identifying highly expressed miRNAs and their targets. UV crosslinking, which is central to these methods, is inefficient and can introduce background. For example, it increases the false discovery rate in genome-wide studies of RNA-protein interactions (Keene et al., 2006). Although use of photoactivatable nucleosides, as in PAR-CLIP, increases the specificity of target identification, it restricts crosslinking to the photoreactive nucleotide, potentially causing sequence bias (Kishore et al., 2011).

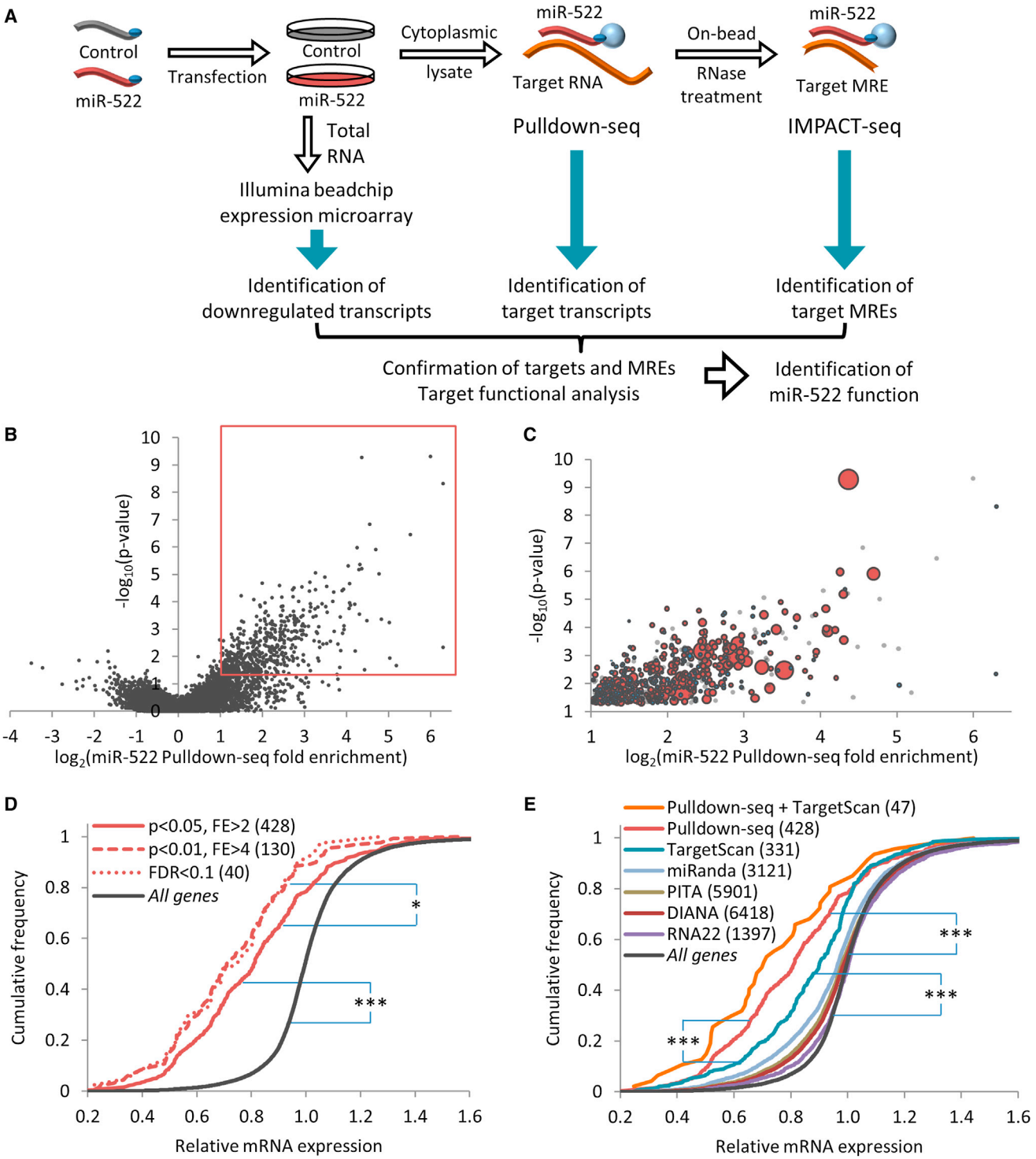

Figure 1. Identification of miR-522 Targets by Pulldown-Seq and Microarray Analysis

(A) Schematic of the strategy used to identify miR-522 target transcripts, MREs, and function.

(B) Volcano plot of gene enrichment in miR-522 versus control Pulldown-seq data set. Red box denotes genes enriched >2-fold with $p < 0.05$.

(C) Bubble plot of genes in the red box in (B). Genes significantly downregulated after miR-522 overexpression by microarray analysis (FDR < 0.1) are in red, those not downregulated are in blue, and those not represented on the microarray are in gray. The size of each bubble is proportionate to the extent of downregulation. Note the higher proportion of red bubbles and larger bubbles with increasing enrichment.

(legend continued on next page)

Bona fide targets for specific miRNAs can be identified without bias by isolating mRNAs bound to a transfected miRNA mimic biotinylated at the 3′ end of the active strand (Lal et al., 2011; Ørom et al., 2008). These transfected miRNA mimics are incorporated into the miRNA-induced silencing complex (miRISC) and bind to and downregulate known mRNA targets. Their association with target mRNAs is not a postlysis artifact, because they do not pull down miRNA targets when added to lysed cells (Lal et al., 2011). These pull-downs do not require crosslinking and can be performed with just a million cells (~20-fold fewer than crosslinking protocols). Typically hundreds to thousands of transcripts are identified as candidate genes regulated by an individual miRNA. Despite these large numbers, the method has high specificity (90% in one study; Lal et al., 2011). However, this method has some shortcomings. Because it uses mRNA microarrays to identify enriched candidate targets, it only identifies mRNAs probed on the array and does not directly identify MREs. Identifying the key miRNA targets and its function(s) from the large network of enriched genes is difficult and relies heavily on gene ontology analysis of target mRNAs. Here, we sought to improve the identification of miRNA targets and function by altering the protocol and subsequent functional analysis to generate a simple, systems-based method for miRNA target characterization (Figure 1A). We replaced the microarray with deep sequencing (Pulldown-seq) and added an RNase step to identify MREs (which we call IMPACT-seq for *i*dentification of *M*REs by *p*ull-down and *a*lignment of *c*aptive *t*ranscripts—*seq*uencing). We also added analysis of the transcription factors that regulate the target genes to gene ontology and interactome analysis of both pulled-down and downregulated genes. These improvements allowed us to identify rapidly key target genes and biological functions of a previously uncharacterized primate-specific miRNA, miR-522.

miR-522 is a member of the chromosome 19 miRNA cluster (C19MC), a 100 kb primate-restricted region that encodes for ~54 tandem miRNAs—the largest miRNA cluster in the human genome. C19MC is highly expressed in human embryonic stem cells and poorly differentiated tumors (Li et al., 2009; Rippe et al., 2010). Members of the cluster, some of which share a common seed, regulate key stem cell genes implicated in cancer, including the Wnt pathway and the tumor-suppressor gene *CDKN1A* (p21Cip1/Waf1; Wu et al., 2010). Thus, C19MC may be an oncogenic miRNA cluster. However, nothing is known about the targets or function of miR-522. Here, we use our new method to discover that miR-522 enhances the ability of triple negative breast cancer (TNBC) cells to survive detachment, invade through a membrane, and express mesenchymal genes, properties associated with metastasis. At the same time, it causes cells to arrest at G1/S, reducing cell proliferation.

RESULTS

miR-522 Is Overexpressed in TNBCs and Other Aggressive Cancers, and Its Amplification Is Associated with Poor Prognosis

Four C19MC miRNAs (miR-517c, miR-519a, miR-521, and miR-522) are overexpressed in TNBCs (Enerly et al., 2011), but only miR-522 is consistently significantly overexpressed in poorly differentiated estrogen receptor (ER)-negative or TNBC, relative to more differentiated ER+ and luminal breast cancers or normal breast tissue, in four additional independent data sets (Biagioni et al., 2012; Buffa et al., 2011; Lowery et al., 2009; Cancer Genome Atlas Network, 2012; Figure S1A). The difference in miR-522 expression between luminal breast cancer and TNBCs was confirmed using ten representative cell lines (Figure S1B).

Identification of miR-522 Target Transcripts by Pulldown-Seq

To identify genes regulated by miR-522, we used the human TNBC cell line MDA-MB-468, which expresses miR-522, as a model system. The RNAs pulled down with biotinylated miR-522 and cel-miR-67 (control miRNA) were compared by RNA sequencing (Pulldown-seq). We obtained 550 and 403 million uniquely aligned bases from two biological replicate experiments, each sequenced in duplicate, from miR-522 and control miRNA samples, respectively, of which about 75% aligned to annotated transcripts. miR-522 target fold enrichment (FE) and p values (p) compared to control miRNA, calculated based on the fragments per kilobase of exon per million fragments mapped (FPKM) of each data set, were depicted in a volcano plot (Figure 1B). Technical validation of 12 randomly selected genes by quantitative RT-PCR (qRT-PCR) confirmed the accuracy of the sequencing data (R^2 = 0.89; Figure S1C). A total of 547 RNAs (mostly mRNAs [85%] but also novel transcripts, pseudogenes, large intergenic noncoding RNAs [lincRNAs], and miRNAs) satisfied the cutoff conditions of FE > 2 and $p < 0.05$ (Figure S1D; Table S1). Depletion of cell lysates with pan-AGO antibody and qRT-PCR analysis of three captured miR-522 target mRNAs showed that Pulldown-seq mostly identified AGO-associated target mRNAs, because the AGO antibody depleted 70%–80% of these targets (Figure S1E).

The mRNA of most bona fide miRNA targets is diminished by miRNA overexpression (Bartel, 2009; Lal et al., 2011). Therefore, to assess the quality of mRNA target identification, Illumina beadchip expression microarrays were used to identify genes downregulated by miR-522 overexpression. The accuracy of the microarray data was confirmed by qRT-PCR analysis of 12 randomly selected genes (R^2 = 0.76; Figure S1F). Of the 547 miR-522 targets, 428 were probed on the microarray and 255 (60%) had significantly downregulated mRNA (false discovery rate [FDR] < 0.1; Figure 1C; Table S1). Cumulative frequency

(D) Cumulative gene expression after miR-522 overexpression, comparing miR-522 targets identified by Pulldown-seq using three different cutoffs. FE, fold enrichment (*K-S test $p < 0.05$; ***$p < 0.001$).

(E) Cumulative gene expression plot comparing miR-522 targets identified by Pulldown-seq (FE > 2; $p < 0.05$) with those predicted by target prediction algorithms (***$p < 0.001$).

See also Figure S1.

plots compared mRNA changes after miR-522 overexpression of genes enriched in the pull-down, defined by different cutoffs, with changes in all genes or algorithm-predicted target genes (Figures 1D and 1E). The decrease in mRNA of the 47 genes selected from the pull-down data using a FDR of <0.1 (40 on the microarray) was similar to the decrease in gene expression of the 197 genes (130 on the microarray) chosen using a cutoff of FE > 4 and $p < 0.01$. The less stringent cutoff (FE > 2; $p < 0.05$) used to define the 547 miR-522 target genes also highly enriched for downregulated mRNAs, outperforming all five algorithm-predicted gene lists (TargetScan, miRanda, PITA, DIANA, and RNA22). Of the algorithms, TargetScan-predicted targets were the most significantly downregulated after miR-522 overexpression (Figure 1E). Pulldown-seq significantly outperformed TargetScan, even though it identified more targets (428 versus 331; $p < 0.001$). Of the 547 candidate target genes, only 53 (47 on the array) were also predicted by TargetScan.

Most miR-522-Associated Genes Had Reduced mRNA and Protein after miR-522 Overexpression

To evaluate the specificity of the pull-down, a random list of 30 genes representing the full range of FE and p values of identified miR-522 targets was chosen. The effect of miR-522 overexpression on mRNA and protein levels was assessed by microarray and immunoblot densitometry, respectively (Figure 2; Table S1). Eighty-three percent (25 of 30) showed significantly reduced mRNA, and 73% (22 of 30) had significantly reduced protein. Thus, Pulldown-seq is very specific for identifying miRNA targets. To test whether endogenous miR-522 suppresses expression of putative Pulldown-seq target genes, we used qRT-PCR to quantify selected target gene mRNAs in cells transfected with anti-miR-522 or a control hairpin. Antagonizing endogenous miR-522 significantly increased three of four miR-522 target mRNAs (*BANF1*, *DHFR*, and *TIMP3*), but not negative control *BRCA1*. Thus, some of the target genes are regulated by endogenous levels of miR-522 (Figure S1G).

Identification of miR-522 Target MREs by IMPACT-Seq

MRE prediction algorithms work best for evolutionarily conserved miRNAs and target sequences. To identify MREs of primate-specific miRNAs, like miR-522, alternate approaches are especially needed. We therefore modified Pulldown-seq to identify MREs, which we call IMPACT-seq. IMPACT-seq requires no crosslinking and only mild RNase T1 treatment of bead-captured miRISCs. cel-miR-67 miRNA was again used as a control to reduce background from RNAs bound nonspecifically to the beads or miRISC. We sequenced and mapped 3.1 and 1.6 million reads uniquely to the genome for control miRNA and miR-522, respectively. Importantly, approximately 65% of all reads had a guanine residue at the 3′ end, indicating that most reads were generated by RNase T1 cleavage. Notably, only 0.7% of the 100,145 reads mapped to other miRNAs (Table S2), indicating that almost all of the sequences captured by IMPACT-seq were associated with miR-522. To identify miR-522 MREs in each sample, we used CLIPper (https://github.com/YeoLab/clipper/), which defines peaks in CLIP experiments. miR-522 peaks were compared to control miRNA peaks and the significance of each potential MRE computed based on a Poisson distribution. The number of normalized reads was also computed for each sample (Table S2). With FE > 2 and $p < 0.05$ cutoffs, we identified 4,848 peaks in 2,966 transcripts with at least five reads in the miR-522 sample as possible MREs.

IMPACT-seq generated sharp, distinct peaks, making it relatively easy to identify MREs with CLIPper or manually using a genome browser (Figure 3A). A large proportion of the RNase-protected sequences (64%) were between 20 and 40 bp, enabling us to identify complementary sequences easily (Figure 3B). Ninety-six percent of miR-522 candidate MREs were located in protein-coding transcripts—53% in the 3′ UTR, 30% in the CDS, and 13% in the 5′ UTR (Figure 3C; Table S2). The remaining sequences aligned to lincRNAs, miRNAs, pseudogenes, and antisense RNAs. Of the 2,467 3′ UTR MREs, only 111 were predicted by PITA, miRanda, and/or TargetScan (Tables S1 and S2).

IMPACT-seq miR-522 targets were also significantly downregulated by miR-522 overexpression but to a lesser extent than Pulldown-seq targets (Figure 3D). The extent of downregulation was similar to the miRanda gene set, but not as good as the TargetScan-predicted genes. Of the 4,848 IMPACT-seq MREs, 743 were in 56% (306 of 547) of Pulldown-seq transcripts. The 275 genes identified by both Pulldown-seq and IMPACT-seq performed comparably to the Pulldown-seq target set (Figure 3D). The lack of MREs for 44% of Pulldown-seq mRNAs and the less-striking downregulation of IMPACT-seq genes suggest that IMPACT-seq could be improved.

To analyze the regions of miR-522 complementarity in these sequences, the GLAM2 tool in the MEME suite of motif-based sequence analysis tools (which allows for gaps or bulges) was used to discover motif(s) (Frith et al., 2008). Reasoning that MREs between 25 and 35 bases in length would contain only single-miR-522-binding sites, we limited analysis to these 1,887 sequences. We found that 1,639 sequences contained an enriched motif partially complementary to residues 13–20 of miR-522 (score: 9,426), and 1,753 contained an enriched motif partially complementary to residues 2–9 in the seed region of miR-522 (score: 9,113). One hundred scrambled versions of the RNase-protected sequences had a significantly lower GLAM2 score of 2,576 ± 1,245 (Figure 3E). Most sequences contained motifs partially complementary to both the 5′ and 3′ ends of miR-522. Thus, miR-522 appears to belong to a recently described class of miRNAs, whose MREs are imperfectly complementary to both miRNA ends (Helwak et al., 2013). Fifty-nine percent of all transcripts containing these GLAM2 motifs were significantly downregulated after miR-522 overexpression. Their cumulative frequency plots were also statistically indistinguishable, supporting our conclusion that miR-522 MREs contain imperfect complementary matches at both ends (Figure 3D; data not shown).

To test the accuracy of IMPACT-seq MRE identification, we cloned a random set of 30 putative MREs (representing the range of read number and FE scores, most of which had a GLAM2 motif) into luciferase reporter plasmids and performed reporter assays (Table S3). Only four were predicted targets and five (17%) had a perfect seed match. Four sequences of similar length that were not identified as MREs, but were encoded in MRE-containing genes, were used as controls. Twenty-five of

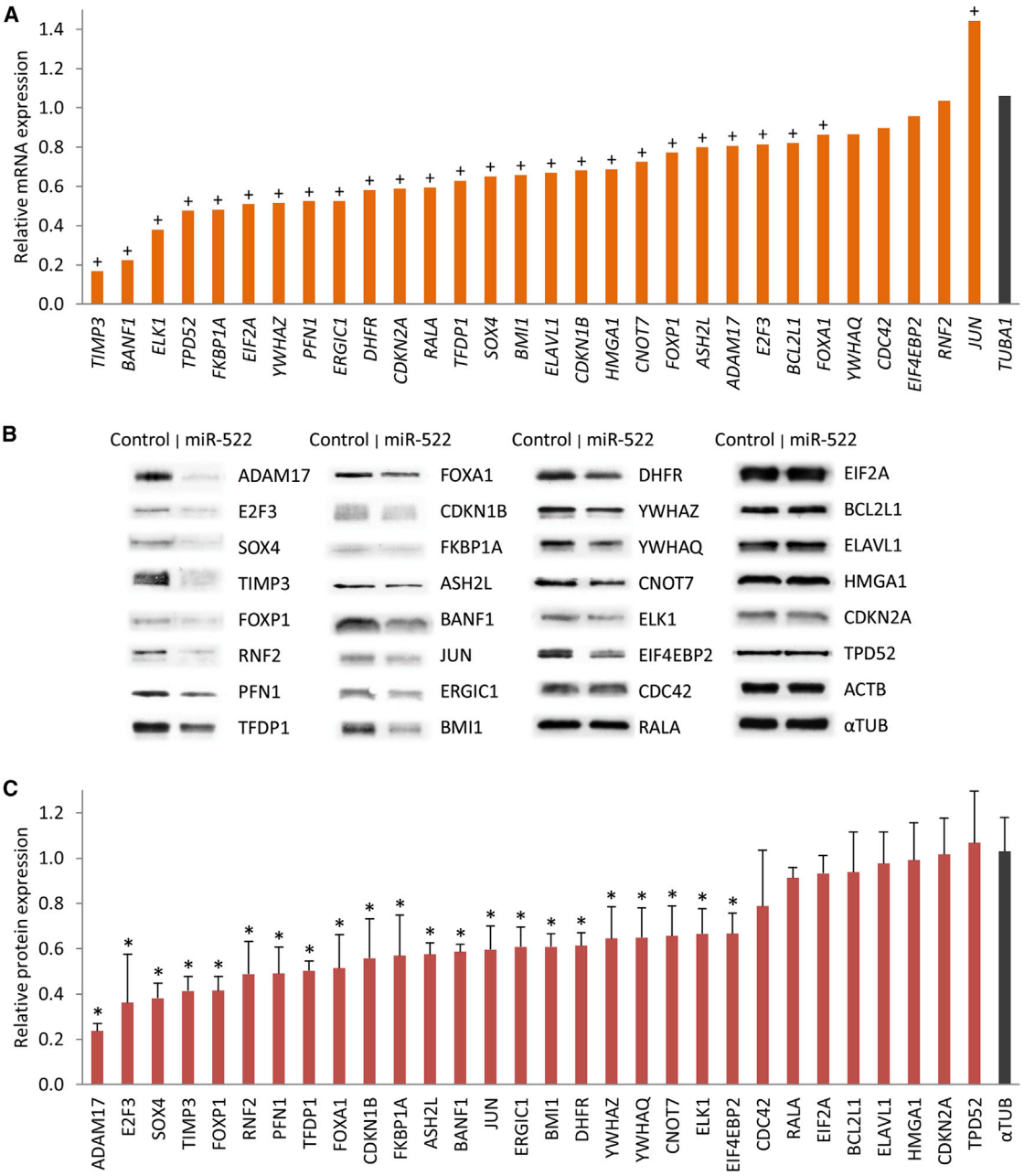

Figure 2. Most miR-522 Pulldown-Seq Targets Have Reduced mRNA and Protein after miR-522 Overexpression

A random set of 30 miR-522 Pulldown-seq targets was analyzed for changes in mRNA and protein expression after miR-522 overexpression.

(A) Microarray analysis of cubic spline-normalized mRNA expression after miR-522 overexpression, compared to control miRNA expression, where + indicates FDR < 0.1.

(B and C) Representative immunoblots (B) and mean ± SD signal intensity relative to β-actin of three independent experiments (C), comparing cells transfected with miR-522 and control miRNA (*p < 0.05, compared to control).

the candidate MREs (83%) reduced luciferase activity (Figure 3F), suggesting that IMPACT-seq is very specific. To confirm that these genes were indeed direct targets of miR-522, we cloned the full-length 3′ UTRs of eight genes with 3′ UTR MREs validated in Figure 3F and performed luciferase reporter assays (Figure 3G). Only one of these did not reduce luciferase activity upon miR-522 overexpression, indicating that most of these MREs function within the endogenous 3′ UTR.

miR-522 Target Functional Analysis

To uncover the function of miR-522, we combined several bioinformatics tools to analyze the Pulldown-seq data set. First, we

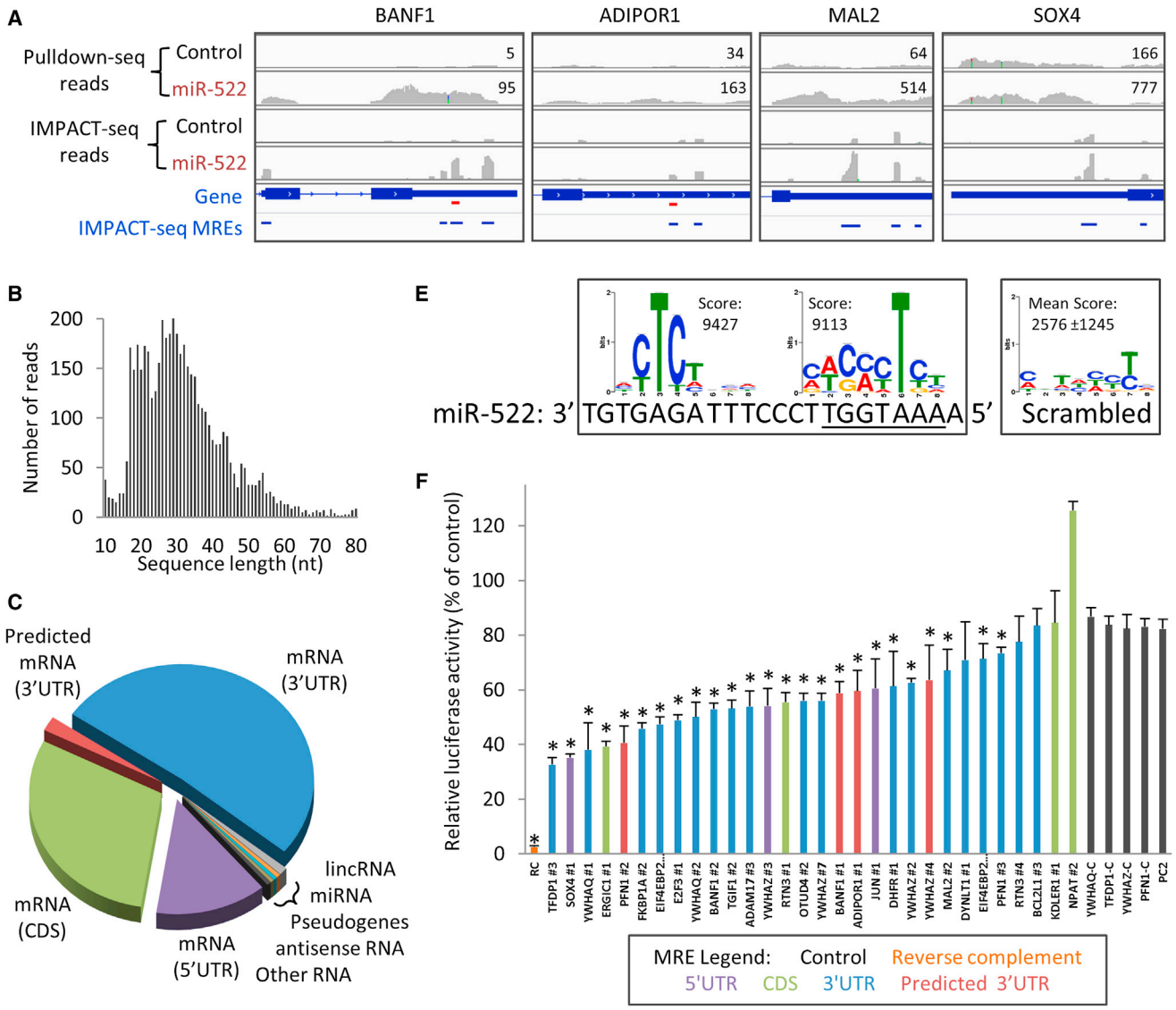

(legend on next page)

used TRANSFAC, a well-curated knowledge base of eukaryotic transcription factors (Matys et al., 2006), to search for overrepresented transcription factors predicted to bind to the promoter regions upstream of miR-522 target genes. Binding sites for four transcription factors, ELK1, E2F, TEAD2, and PAX3, which are all expressed in MDA-MB-468, were significantly enriched in the promoters of the 547 Pulldown-seq genes (Figure 4A). *ELK1* and *E2F3* were also identified as miR-522 target genes that were enriched 17- and 2.8-fold in the pull-down, respectively. The mRNA and protein levels of both were significantly downregulated by miR-522 overexpression (Table S1; Figure 2). ELK1 and PAX3 both enhance the epithelial state. ELK1-regulated genes are downregulated during transforming growth factor β (TGF-β)-induced epithelial mesenchymal transition (EMT) (Venkov et al., 2011), whereas PAX3 expression enhances mesenchymal epithelial transition (MET) (Wiggan et al., 2002). Of note, TEAD2 transcriptionally activates PAX3 (Milewski et al., 2004). This analysis suggests that miR-522 might foster EMT. E2F transcription factors promote G1/S progression in the cell cycle (Fan and Bertino, 1997), suggesting that miR-522 might inhibit progression at this phase of the cell cycle.

miRNAs can target multiple genes that participate in common pathways (Lal et al., 2009, 2011). We therefore next used ingenuity pathway analysis (IPA), which curates biological interactions and function (Ingenuity Systems; http://www.ingenuity.com), to identify all directly related miR-522 target genes (Figure S2). This interactome of 221 genes was then analyzed using IPA to identify the top network-associated functions (Figure 4B). These included cellular movement and morphology (functional components of EMT), embryonic development (of which EMT is an essential component), as well as cell cycle, corroborating the TRANSFAC analysis. To include possible indirect functional effects of miR-522, we next identified common molecular functions overrepresented in both the Pulldown-seq interactome and set of 205 directly connected genes whose mRNAs were significantly downregulated after miR-522 overexpression ($p < 0.0001$ and fold change > 1.5; Table S4). The p values for each common overrepresented molecular function were displayed in a bubble plot, where the number of miR-522 target genes identified by Pulldown-seq for each function is proportional to the bubble size (Figure 4C). The most significantly enriched functions, for which more than ten target genes were annotated, fell into four large functional categories: proliferation, apoptosis, cell cycle, and cell morphology/migration/transformation. The latter two categories also stood out in both the TRANSFAC and IPA analyses. Based on these bioinformatics, we hypothesized that miR-522 might regulate G1/S cell cycle progression, cell transformation and survival, cell motility, and EMT, which we next investigated in MDA-MB-468 TNBC cells.

miR-522 Overexpression Induces Mesenchymal Properties

Loss of cellular adhesion is an easily detectable phenotype that involves changes in cell morphology, movement, and cytoskeletal organization and is an important step in EMT (Yang and Weinberg, 2008). In tissue culture, most MDA-MB-468 cells are adherent, but some detach and remain viable. We first assessed by TaqMan PCR whether miR-522 levels might be different in adherent versus nonadherent cells. miR-522 was expressed at significantly higher levels in nonadherent than adherent cells, but another C19MC miRNA (miR-519a), miR-16, and let-7a were expressed similarly (Figure 5A). Overexpression of miR-522 decreased the number of live adherent cells and increased the number of live cells in suspension (Figure 5B). To assess whether miR-522 expression was responsible for loss of adhesivity, we collected suspension cells that were transfected 48 hr previously with either control miRNA or miR-522 and retransfected an equal number of each with control miRNA, miR-522, or anti-miR-522. Only cells transfected with anti-miR-522 formed adherent colonies (Figure 5C). Thus, miR-522 promotes detachment and viability of detached cells.

We next investigated whether miR-522 promotes EMT. Changes in important mesenchymal gene (*ZEB2*, *TWIST1*, *FOXC2*, *SNAI1*, *SNAI2*, and *VIM*) transcripts were assessed by qRT-PCR in adherent and nonadherent cells 3 and 5 days after miR-522 or control miRNA transfection (Figures 5D and 5E). Expression of all six genes strongly and progressively increased in both cell populations but most dramatically in nonadherent cells. However, epithelial genes encoding E-cadherin (*CDH1*) or the cytokeratins (*KRT14*, *KRT18*, and *KRT19*) did not significantly change (Figure S3A). These results are consistent with the notion that poorly differentiated cancer cells exhibit plasticity in epithelial and mesenchymal properties and can simultaneously show features of both states (Granit et al., 2013). Overexpression of miR-522, and to a lesser extent miR-517c, but not the other two C19MC miRNAs abundant in TNBCs (Enerly et al.,

Figure 3. Identification of miR-522 MREs by IMPACT-Seq

(A) Sequencing reads of four miR-522 targets and MREs. Numbers in Pulldown-seq plots indicate mean FPKM (scale: Pulldown-seq 0–100 reads, IMPACT-seq 0–50 reads). IMPACT-seq-identified MREs are indicated below in blue; two of these also predicted by Miranda are shown in red.

(B) Lengths of sequences containing identified miR-522 MREs. Most MRE-containing sequences were between 20 and 40 nt.

(C) Distribution of miR-522 MREs among RNA classes. The majority of predicted MREs were in the 3′ UTR of mRNAs.

(D) Cumulative gene expression plot comparing miR-522 targets identified by IMPACT-seq and/or Pulldown-seq with those predicted by target prediction algorithms (***K-S test $p < 0.001$).

(E) GLAM2 gapped motif analysis of 1,887 MREs between 25 and 35 nt shows enrichment of a 3′ supplementary motif in 1,639 MREs and a noncanonical seed match in 1,753 MREs (left box, seed sequence underlined). GLAM2 analysis for 100 iterations of scrambled sequences of the same MREs resulted in motifs with significantly lower mean score ± SD (representative motif shown in the right box).

(F) Dual luciferase assay of 30 randomly selected MREs. RC indicates the miR-522 reverse complement sequence used as positive control, C indicates negative control sequences not bound by miR-522, and PC2 denotes the empty vector. Twenty-five of 30 MREs were functional by luciferase assay. Mean ± SD of three independent experiments (*$p < 0.05$ compared to control).

(G) Dual luciferase assay of eight full-length 3′ UTRs with verified miR-522 MREs in (F), using the same positive and negative controls. Seven of eight were regulated by miR-522. Mean ± SD of three independent experiments (*$p < 0.05$ compared to control).

A

Transcription factor	p-value	Motif	Number of genes	Function
ELK1	1.77×10^{-5}	CCGGAART	113	Regulates cytoskeleton and migration Identified here as a target of miR-522 Targets downregulated upon EMT
E2F	9.83×10^{-5}	GGCGSG	281	Regulator of G1/S cell cycle progression E2F3 identified here as a target of miR-522
TEAD2	8.40×10^{-4}	GVGGMGG	184	Hippo signaling transcriptional regulator Positive regulator of PAX3
PAX3	3.76×10^{-3}	CGTCACGSTY	101	Developmental regulator Positive regulator of MET

B

Top associated network functions	IPA score
Cellular movement, embryonic development, cell morphology	71
Gene expression, cell cycle, connective tissue development and function	44
Cell signaling, connective tissue disorders, developmental disorder	35
Cellular movement, hematological system development and function, immune cell trafficking	32
Cardiovascular system development and function, embryonic development, organ development	17

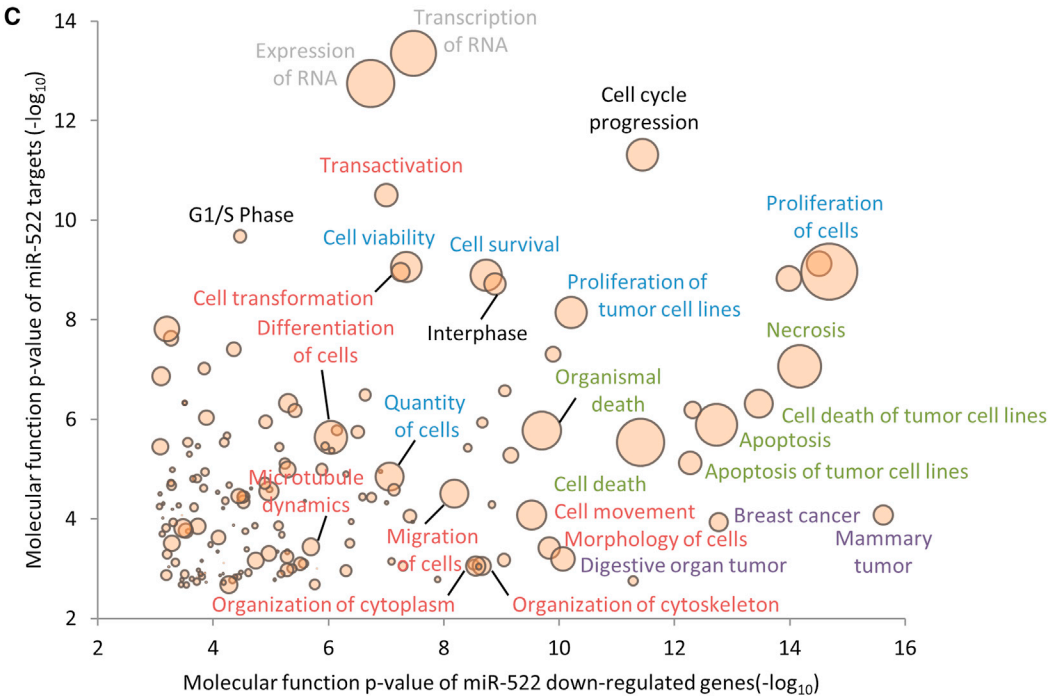

Figure 4. Bioinformatics Analysis of miR-522 Target Genes

(A) Promoter regions of miR-522 target genes that were enriched for binding sites of four transcription factors by TRANSFAC analysis.

(B) Top enriched functions of directly associated miRNA-522 targets by IPA. Score: $-\log_{10}$(p value). EMT-related functions are indicated in red.

(C) Bubble plot of the IPA molecular function p values of directly associated miR-522 targets plotted against interactome genes that were downregulated by miR-522 overexpression (IPA $p < 0.0001$; FC > 1.5). The size of each bubble is proportional to the number of miR-522 target genes assigned to that molecular function. Bubbles are selectively annotated based on low p values and large size and annotated by function: cell cycle (black), proliferation (blue), cell death (green), cancer (purple), EMT-related (cell morphology, movement, transformation, and differentiation: red), and others (gray).

See also Figure S2.

2011), induced EMT marker expression. These miRNAs functioned differently, even though they have strikingly similar sequences (Figure S3B).

EMT is linked to cancer stem cells, invasion, and metastasis. A small, but significant, increase in the stem/early progenitor cell genes, *CD44* and *CD133*, was also seen (Figure S3A). $CD44^{+}/CD24^{low/-}$ expression enriches for cancer stem cells. Although most MDA-MB-468 cells are already CD44+, miR-522 overexpression reduced CD24 levels (Figures S3C and S3D). Both transient and stable miR-522 overexpression significantly increased migration through a membrane by 4- to 5-fold compared to control cells. More cells migrated and adhered to the membrane or survived in suspension in the lower chamber (Figures 5F–5I and S3E). Thus, miR-522 overexpression promotes important EMT hallmarks.

miR-522 Overexpression Causes G1/S Arrest

We next used propidium iodide staining to examine the effect of miR-522 on the cell-cycle profile of MDA-MB-468 and HCC1937 TNBC cells. miR-522 overexpression significantly increased the number of cells in the G1 phase and correspondingly decreased cells in S and G2/M, compared to control miRNA (Figures 5J, 5K, S3F, and S3G). These results confirm the bioinformatics analysis.

Target Gene Knockdown Partially Recapitulates miR-522 Overexpression Phenotype

To test the importance of individual target genes, we chose for further study 21 genes in the Pulldown-seq data set that function in adhesion (matrix metalloproteinase inhibitor *TIMP3*, focal adhesion regulator *ZFYVE21*, cell-matrix regulator *YWHAZ*, developmental transcription factor and cell adhesion regulator *HOXA1*, and epithelial cell adhesion regulator *PFN1*); EMT (genes whose knockdown induces EMT—*SPSB1*, *ADAM17* [Liu et al., 2009], *FOXA1* [Song et al., 2010], and *DEDD2* [Lv et al., 2012]—or which repress TGF-β signaling—*FKBP1A*, *TGIF1*, *TGIF2*, and *ELK1*); or cancer or stem cell biology (tumor suppressors *FOXP1* and *DNAJC25*, breast cancer-amplified tumor gene *TPD52*, cycling membrane protein *ERGIC1*, polycomb group genes *BMI1* and *RNF2*, Ccr4-NOT deadenylase subunit *CNOT7*, and antifolate drug target *DHFR*). We first asked whether knockdown of these genes individually recapitulated miR-522's ability to promote detachment without anoikis. Each of these genes was knocked down at least 3-fold, except for *TGIF1*, whose expression was reduced 2-fold (Figure S4). Knockdown of 10 of the 21 genes, including all five adhesion-related genes and half of the EMT-related genes, significantly decreased the number of attached viable cells 3 days later (Figure 6A). However, knockdown of only three of these (*ZFYVE21*, *TIMP3*, and *SPSB1*) also increased the number of live cells in suspension (Figure 6B). Knockdown of four other genes (*FOXA1*, *DEDD2*, *TPD52*, and *BMI1*) only increased the number of viable nonadherent cells.

Next, we examined by qRT-PCR whether individual knockdown of any of the 21 genes enhanced expression of the mesenchymal transcription factors *ZEB2*, *FOXC2*, and *SNAI2* upregulated by miR-522 (Figure 6C). Knocking down *TIMP3*, *PFN1*, *FOXA1*, *TGIF2, SPSB1*, or *BMI1* upregulated all three transcription factor mRNAs 5 days later, although less potently than miR-522 overexpression. These data suggest that miR-522 regulates invasivity and mesenchymal gene expression by suppressing the expression of multiple genes identified by Pulldown-seq.

DISCUSSION

Identifying miRNA targets and function is challenging, requiring a lot of trial and error (Thomas et al., 2010). This is especially true of nonconserved miRNAs and miRNAs that recognize their targets by noncanonical binding. Here, we describe a relatively straightforward systems-based strategy for miRNA target gene identification and functional characterization. We used it to identify miR-522 target genes, MREs, and function, directly and readily, with a high degree of specificity. Although identified MREs did not follow canonical rules, most target genes had reduced mRNA and protein levels when miR-522 was overexpressed, and most identified MREs tested were active by luciferase assay (Figure 7A). The method is simple and can be performed with only a million cells. Other advantages include freedom from assumptions about target recognition rules, reduced sequence biases from crosslinking, direct genome-wide identification of regulated mRNAs and MREs, and the ability to identify noncoding transcripts as miRNA targets. Functional miRNAs are associated with all four AGO homologs (Hafner et al., 2010; Su et al., 2009). Our method identifies miRNA targets and MREs, regardless of which AGO protein(s) are involved. Combining biotinylated miRNA pull-down with AGO immunoprecipitation might improve target identification and could be used to investigate whether individual AGOs obey distinct binding rules.

We added TRANSFAC promoter analysis to more commonly used bioinformatics tools (interactome and gene ontology functional analysis) to analyze both pulled-down and downregulated genes to facilitate the tricky task of identifying the biological function of a previously unstudied miRNA. This bioinformatics work flow led to robust predictions of miR-522 function that directed experimental efforts into fruitful investigations and avoided unproductive searching. This streamlined approach should be useful for uncovering the hidden meaning of large genome-wide data sets.

Recent studies have suggested that individual miRNAs differ in how they recognize their targets. miR-522 recognizes its mRNA targets largely by binding to both an imperfect seed match and a 3′ supplementary motif. In fact, globally noncanonical binding may be more prevalent than canonical seed pairing (Loeb et al., 2012; Xia et al., 2012). Seed-only interactions were found in fewer than one in five endogenous miRNA-MRE pairs identified by CLASH (Helwak et al., 2013). The experimentally verified miR-522 MREs were located in the CDS and 3′ and 5′ UTRs of target mRNAs, corroborating previous studies that MREs occur outside the 3′ UTR (Lal et al., 2011; Tay et al., 2008). Although the 3′ UTR was overrepresented and was where most (56%) MREs were located, this is only a modest overrepresentation, because 3′ UTRs make up 43% of RefSeq sequences. The PAR-CLIP data set also reported moderate genome-wide overrepresentation of MREs in the 3′ UTR (Hafner et al., 2010).

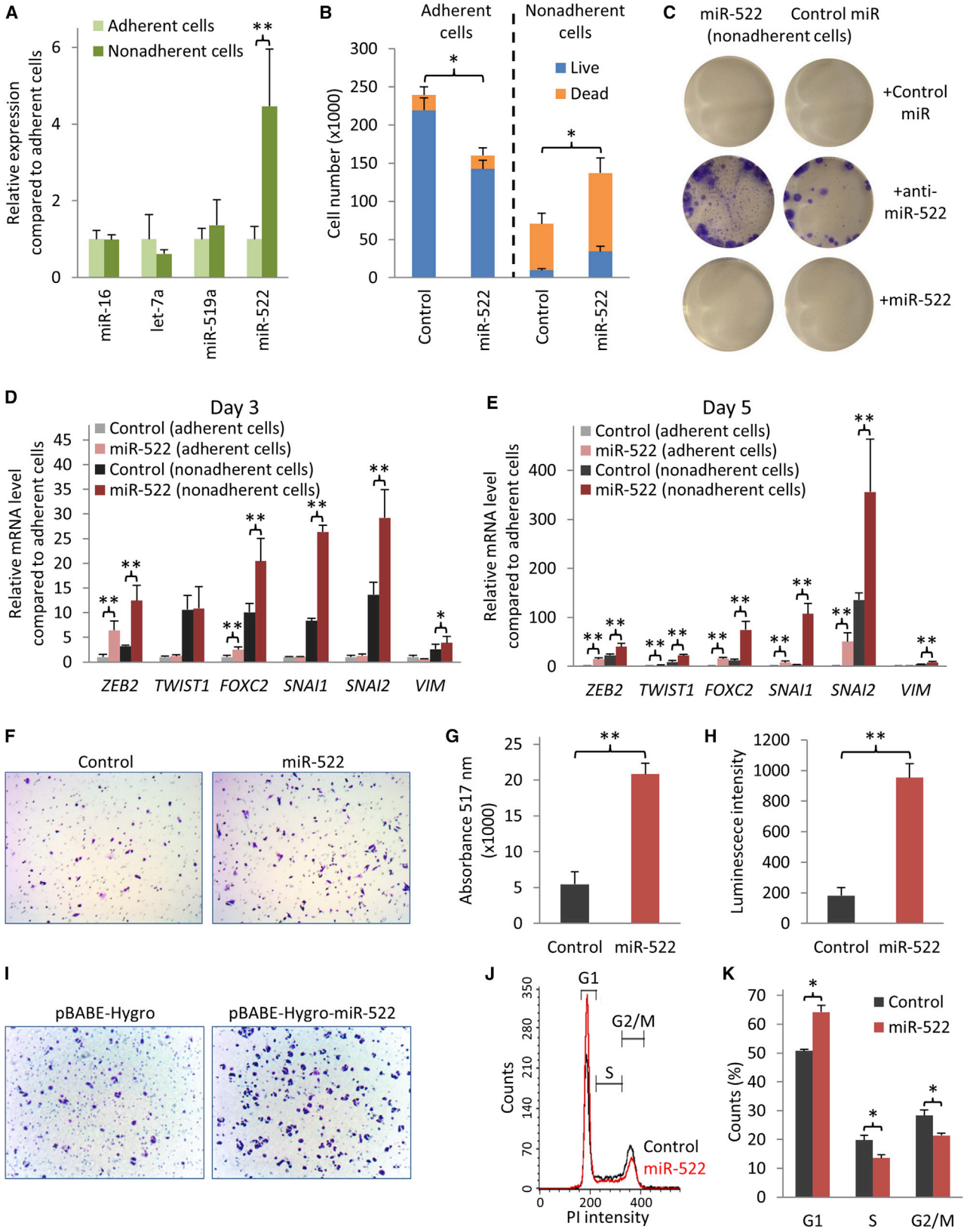

(legend on next page)

The cutoffs chosen to define targets are somewhat arbitrary. Increasing the stringency reduces false positives but also reduces the sensitivity for identifying bona fide targets. For example, changing the fold enrichment cutoff in the pull-down from 2 to 4 significantly improved the cumulative gene expression plot but at the cost of dramatically reducing the number of candidate targets by about a third. However, the most important targets, those most downregulated by miR-522, may be more enriched in the pull-down (Figure 1D). With our current cutoffs, we identified more potential miR-522 targets with IMPACT-seq than with Pulldown-seq. This apparent discrepancy can be explained by the fact that IMPACT-seq looks at a much-smaller sequence window. If a transcript contains MREs for both control miRNA and miR-522 in different locations, Pulldown-seq will not identify this transcript as a target unless it is pulled down with different efficiencies (1,704 transcripts have at least one MRE in both control and miR-522). However, we identified MREs for more than half of the miR-522 target transcripts, an impressive statistic considering that the data sets were generated from distinct experiments using two different sequencing platforms. To improve the overlap of regulated mRNAs and MRE-containing transcripts, the stringency of Pulldown-seq cutoffs could be relaxed and/or the sequencing coverage of IMPACT-seq could be improved. With our current method and cutoffs, we view these two methods of identifying miRNA targets as complementary.

miR-522 caused G1 cell-cycle arrest and loss of adhesion without anoikis and induced mesenchymal genes and properties in a TNBC cell line (Figure 7B). Acquisition of mesenchymal properties is thought to promote cancer progression and metastasis, especially in breast cancer (Yang and Weinberg, 2008). Although miR-522 induced mesenchymal genes and mesenchymal properties, it did not downregulate epithelial gene expression in this cell line. Breast cancer circulating tumor cells (CTCs), which are thought to be the intermediary between primary tumor and secondary metastatic cells, highly express mesenchymal markers even though most primary solid tumors and their metastases are epithelial (Aktas et al., 2009; Kallergi et al., 2011). However, breast cancer CTCs, like the miR-522-overexpressing cells in this study, often coexpress epithelial and mesenchymal genes. In fact, CTCs in mice implanted with metastasizing MDA-MB-468 xenographs express both mesenchymal genes and epithelial E-cadherin (Bonnomet et al., 2012). Rather than undergoing an EMT, it might be more accurate to characterize metastasizing cancer cells as occupying a metastable state between these two fixed lineages. Expression of miR-522 may turn on this metastatic program to increase motility, survival, and numbers of CTCs. Supporting our hypothesis that miR-522 instigates metastasis, miR-522 was more highly expressed in CTCs from patients with TNBC tumors that are prone to metastasize than in better prognosis ER+ tumors (Sieuwerts et al., 2011). There is currently no targeted therapy for TNBC, the breast cancer with the worst prognosis. In the future, miR-522 antagonists could be evaluated for treating TNBC patients, especially for tumors with amplified C19MC.

Several miRNAs, including miR-200, miR-205, and miR-34, induce epithelial transition (Lamouille et al., 2013). Some of these induce this dramatic change in cellular state by suppressing key transcriptional activators of mesenchymal genes, such as *Snai1* and *Snai2*, or transcriptional repressors of epithelial genes, such as *Zeb1*/*Zeb2*. More recently, miRNAs, such as miR-9, miR-22, and miR-661, have been identified that accomplish the reverse—reduce expression of epithelial genes and induce mesenchymal programs (Ma et al., 2010; Song et al., 2013; Vetter et al., 2010). miR-22 targets the TET family of methylcytosine dioxygenases that may globally suppress epithelial gene expression indirectly by inhibiting demethylation of miR-200 family promoters, thereby suppressing *Zeb* expression. Some of the mesenchymal-promoting miRNAs suppress the expression of one or two epithelial genes, such as genes encoding E-cadherin (miR-9) or nectin-1 (miR-661), which help maintain tight junctions. However, modulation of a single target rarely explains most of a miRNA's effect. Many miRNAs target multiple transcripts in the same networks or pathways to regulate biological processes. An apt analogy might be transcription factors, which regulate many genes; one regulated gene rarely reproduces the effect of the transcription factor. Thus, miRNAs regulate the epithelial-mesenchymal transitions most likely by targeting other genes in the key pathways that contribute to this transition, as we found for miR-522. In fact, a miR-200 pull-down (R. Perdigão-Henriques, F. Petrocca, G. Altschuler, M.P. Thomas, M.T.N. Le, S.M.T., W.H., and J.L., unpublished data) identified miR-200 target genes that interact with Zeb transcription factors to

Figure 5. Overexpression of miR-522 Induces Hallmarks of Epithelial-Mesenchymal Transition

(A) qRT-PCR analysis of miRNA levels in MDA-MB-468 cells showed a higher level of miR-522 in nonadherent cells. Mean ± SD of three independent experiments (**$p < 0.01$ compared to control).

(B) Trypan blue exclusion cell counts of adherent and nonadherent cells 3 days after transfection with miR-522 or control miRNA showed a higher number of miR-522-transfected live cells in suspension. Mean ± SD of three independent experiments (*$p < 0.05$ compared to control).

(C) Nonadherent cells transfected with control or miR-522 as in (B) were retransfected with anti-miR-522, control antisense miRNA, or miR-522. Only antagonizing miR-522 led to adherent colonies (representative photos).

(D and E) qRT-PCR analysis of EMT genes, normalized to *GAPDH*, in adherent and nonadherent cells 3 (D) and 5 (E) days after transfection with miR-522 or control miRNA. Note the difference in the scales. Mean ± SD of three independent experiments (*$p < 0.05$; **$p < 0.01$ compared to control).

(F–H) Transwell invasion assay demonstrates that transient miR-522 overexpression increases invasion. (F) Representative photos of crystal violet-stained invading cells. (G) Quantification by calcein AM staining. (H) Quantification of invaded live cells in suspension in the bottom chamber by CellTiter-Glo. Mean ± SD of three independent experiments (**$p < 0.01$ compared to control).

(I) Transwell invasion assay as in (F) but with MDA-MB-468 cells stably infected with pBABE-Hygro or pBABE-Hygro-miR-522.

(J and K) Cell-cycle analysis of MDA-MB-468 cells transfected with miR-522 or control miRNA, showing an increase in cells in the G1 phase. (J) shows a representative profile. (K) shows mean ± SD of three independent experiments (*$p < 0.05$ compared to control). PI, propidium iodide.

See also Figure S3.

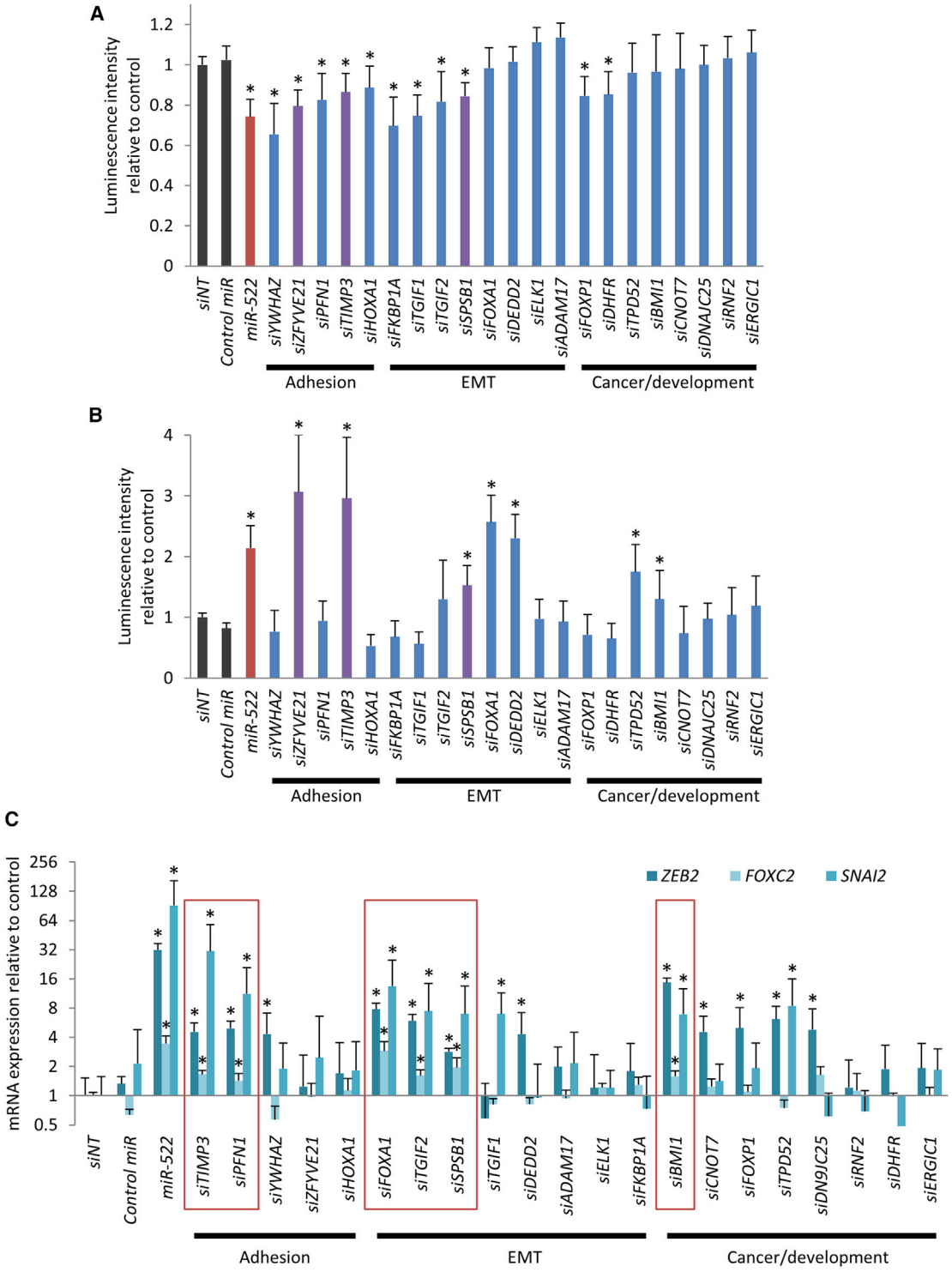

Figure 6. Knockdown of Individual Target Genes Partly Recapitulates Effects of mir-522 Overexpression

(A and B) CellTiter-Glo was used to quantify live adherent (A) and nonadherent cells (B) 3 days after small interfering RNA (siRNA) or miRNA transfection, normalized to nontargeting siRNA control (siNT). Bars in purple indicate genes whose knockdown both decreased live adherent cells and increased live nonadherent cells. (C) qRT-PCR analysis of relative EMT gene mRNA in adherent cells 5 days after siRNA or miRNA transfection. Relative mRNA level normalized to *GAPDH* was compared to cells transfected with siNT. Knockdown of genes in the red boxes significantly enhanced the expression of all three mesenchymal transcription factors. Mean ± SD of three independent experiments (*$p < 0.05$; compared to control).

See also Figure S4.

A

Test experiment	Tested	Positive	Positive rate
Transcript down-regulation	428	255	59.6%
Protein down-regulation	30	22	73.3%
3′UTR MRE luciferase assay	30	25	83.3%

B

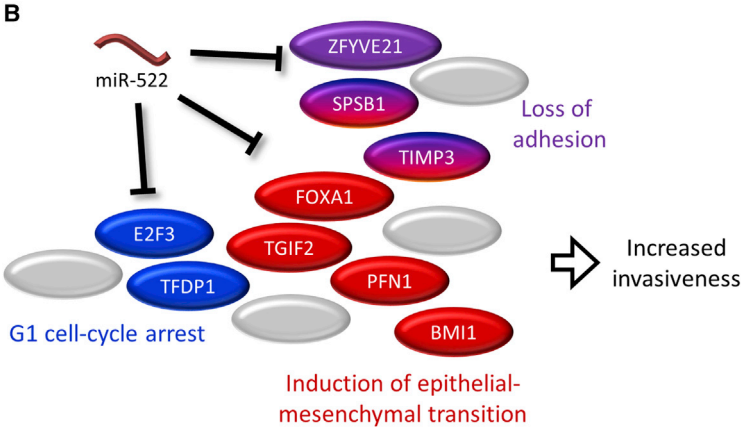

Figure 7. Model of miR-522 Functions

(A) Summary of experimental results to validate the specificity of Pulldown-seq and IMPACT-seq for identifying miR-522 target mRNAs and MREs.

(B) Schematic showing important miR-522 targets and their biological functions.

suppress epithelial genes. The advantage of Pulldown-seq is its ability to identify without bias bona fide miRNA targets. Our results suggest that miR-522 targets a large number of transcripts, of which probably only a subset are biologically important in a given cell at a particular time. It will be worthwhile to define at a systems level the genes regulated by the EMT- and MET-regulating miRNAs. The method described here should be useful for accomplishing this goal.

EXPERIMENTAL PROCEDURES

Cell Culture and Transfection

Breast cancer cell lines were obtained from American Type Culture Collection and cultured as recommended. Unless otherwise stated, DharmaFECT 1 reagent (Dharmacon) was used for transfection. Control miRNA (cel-miR-67) or miR-522 mimic (50 nM, Thermo Scientific) was used to transfect 100,000 cells/well in suspension in 12-well dishes as per manufacturer's protocol, and medium was changed after 24 hr.

Microarray

Total RNA, extracted using Trizol (Invitrogen) 48 hr after transfection from biological triplicate wells, was purified with the RNeasy kit (QIAGEN). cDNA and cRNA were generated and hybridized to HT-12 v4 beadchips (Illumina) according to the manufacturer's protocols. Cubic spline-normalized (without background normalization) data were analyzed by the NIA Array Analysis tool (http://lgsun.grc.nia.nih.gov/ANOVA) to identify transcripts downregulated after miR-522 overexpression.

Pulldown-Seq

MDA-MB-468 pull-down experiments with control miRNA (cel-miR-67) and miR-522 mimic (Thermo Scientific) were conducted as described previously but modified to include molecular crowders in the lysis buffer (Lal et al., 2011; Tan et al., 2014). Briefly, cell pellets were collected 24 hr posttransfection, washed twice with cold PBS, and incubated with lysis buffer (20 mM Tris [pH 7], 25mM EDTA [pH 8], 100 mM KCl, 5 mM $MgCl_2$ [all Ambion], 2.5 mg/ml Ficoll PM400, 7.5 mg/ml Ficoll PM70 [GE Healthcare], 0.25 mg/ml dextran sulfate 670k, 0.3% NP-40 [Fluka], 50 U each of RNase OUT and SUPERase In [Invitrogen], and complete protease inhibitor cocktail [Roche Applied Science]) on ice for 20 min. The cytoplasmic lysate, isolated by centrifugation at 5,000 g for 5 min, was added to 1 mg/ml yeast tRNA and 1 mg/ml BSA (Ambion)-blocked streptavidin (SA)-coated magnetic beads (Invitrogen) and rotated for 4 hr at 4°C. The beads were washed five times with 1 ml lysis buffer and bead-bound RNA extracted using Trizol LS (Invitrogen). Ribosomal RNA was depleted using the Ribo-Zero rRNA removal kit (Epicenter). Libraries were generated using the NEBNext Multiplex Small RNA Library Prep Set with modified adaptors and primers compatible for Ion Torrent Sequencing Platform (New England Biolabs) and sequenced on the Ion Torrent platform using the 314 Chip (Invitrogen), according to the manufacturer's protocols.

IMPACT-Seq

The IMPACT-seq protocol used the Pulldown-seq protocol to isolate miRNA-bound RNAs with SA beads as above. The cytoplasmic lysate-SA bead mixture was incubated with rotation overnight at 4°C before adding RNase T1 (25 U/μl) for 10 min on-bead digestion at 37°C. RNA was then extracted from washed beads using Trizol LS as above. The RNA was treated with T4 Polynucleotide Kinase (NEB) to obtain 5′-phosphate ends for subsequent ligations and then passed through NucAway columns (Ambion) to remove RNAs <20 nt in length. Libraries were generated using the NEBNext Small RNA Sample Prep Set for Illumina chemistry (NEB). cDNA fragments with an insert size of 20–60 nt were gel extracted and sequenced on the HiSeq platform (Illumina) according to the manufacturer's protocol.

RNA-Seq Quality Control and Alignment

Prealignment and postalignment libraries were screened for quality, specificity of mapping, and contaminant sequences using FASTQC (http://www.bioinformatics.babraham.ac.uk/projects/fastqc/), RSeQC (Wang et al., 2012), and RNA-SeQC (DeLuca et al., 2012). Prior to alignment, low-quality bases, homopolymer sequences, sequences matching the first 13 bp, and the reverse complement of the adaptor sequences for IonTorrent or Illumina were trimmed using cutadapt version 1.2.1 (Martin, 2011). Trimmed reads smaller than 30 nt for Pulldown-seq or 20 nt for IMPACT-seq were discarded. Pulldown-seq used reads that uniquely mapped to the GRCh37 assembly of the human genome augmented with the Ensembl 68 genome annotation using Novoalign (http://www.novocraft.com) with the following parameters: -H -k -n 250 -F STDFQ -r all 10 -e 10 -g 15 -x 4. IMPACT-seq used reads that uniquely mapped (with greater than or equal to two mismatches) to the GRCh37 assembly of the human genome augmented with the Ensembl 72 genome annotation (Flicek et al., 2013), using Tophat version 2.0.8b (Trapnell et al., 2009). Quality control, trimming, and alignment were performed using the bipy (https://github.com/roryk/bipy) and bcbio-nextgen (https://github.com/chapmanb/bcbio-nextgen) automated sequencing analysis pipelines.

Pulldown-Seq Target Identification

Postalignment gene counts were generated using htseq-count 0.5.4p3 with the counts aggregated by gene_id of the Ensembl 68 annotation. Differentially expressed transcripts were called with DESeq version 1.9.2 using the default options (Anders and Huber, 2010). The top hits with FE > 2 and $p < 0.05$ were flagged as candidates for downstream biological verification.

IMPACT-Seq MRE Identification

Peaks were called on both control miRNA and miR-522 IMPACT-seq samples using CLIPper (https://github.com/YeoLab/clipper/) with the following

parameters: –poisson-cutoff = 0.05–superlocal–max_gap = 0–processors = 8 -b $file -s hg19 -o $file. MREs were identified by requiring that the peak have greater than or equal to five reads in the miR-522 sample with at least twice as many normalized reads in the miR-522 sample as control.

Target Functional Analysis

We first identified possible common transcription-factor-binding sites in all miR-522 target genes identified by Pulldown-seq with TRANSFAC (http://www.gene-regulation.com), using the default settings. We then used IPA (http://www.ingenuity.com) to connect all miR-522 target genes that were directly related with the default settings, as defined by the curated IPA database, without selecting the optional predicted miRNA interactions. This list of genes was then subject to a core analysis with the default IPA settings, to generate a list of IPA scores for the top associated network functions and significantly enriched molecular functions. We then performed a similar IPA core analysis on directly related genes that were significantly downregulated after miR-522 overexpression. A list of the significantly enriched molecular functions shared by the Pulldown-seq and downregulated gene interactomes was used to identify common functions.

Statistical Analysis

In vitro data were analyzed using unpaired Student's t test; cumulative distribution plots were analyzed using the Kolmogorov-Smirnov test (K-S test). $p < 0.05$ was considered significant. *$p < 0.05$; **$p < 0.01$; ***$p < 0.001$. The mean ± SD of three or more independent experiments is reported.

ACCESSION NUMBERS

Pull-down, IMPACT RNA-seq, and overexpression microarray datasets are available in the ArrayExpress database (http://www.ebi.ac.uk/arrayexpress) under accession numbers E-MTAB-2112, E-MTAB-2119, and E-MTAB-2110, respectively.

SUPPLEMENTAL INFORMATION

Supplemental Information includes Supplemental Experimental Procedures, four figures, and four tables and can be found with this article online at http://dx.doi.org/10.1016/j.celrep.2014.07.023.

AUTHOR CONTRIBUTIONS

S.M.T. and J.L. designed the experiments, analyzed the data, and wrote the manuscript. S.M.T. performed the experiments. J.J. and L.M. obtained the RNA-seq data. R.K., O.H., and W.H. did the bioinformatics analysis.

ACKNOWLEDGMENTS

We thank J.L. laboratory members for critical discussions. S.M.T. is supported by the Department of Defense Breast Cancer Research Program. Microarray experiments were performed by the Molecular Genetics Core Facility at Boston Children's Hospital supported by NIH-P50-NS40828 and NIH-P30-HD18655. The bioinformatics analyses, supported by the HSCI Center of Stem Cell Bioinformatics, were run on the Odyssey cluster supported by the Harvard University FAS Research Computing Group. J.J. and L.M. are employees of New England Biolabs, a company that sells deep sequencing kits for RNA and DNA research.

Received: November 21, 2013
Revised: May 7, 2014
Accepted: July 16, 2014
Published: August 14, 2014

REFERENCES

Aktas, B., Tewes, M., Fehm, T., Hauch, S., Kimmig, R., and Kasimir-Bauer, S. (2009). Stem cell and epithelial-mesenchymal transition markers are frequently overexpressed in circulating tumor cells of metastatic breast cancer patients. Breast Cancer Res. *11*, R46.

Anders, S., and Huber, W. (2010). Differential expression analysis for sequence count data. Genome Biol. *11*, R106.

Bartel, D.P. (2009). MicroRNAs: target recognition and regulatory functions. Cell *136*, 215–233.

Biagioni, F., Bossel Ben-Moshe, N., Fontemaggi, G., Canu, V., Mori, F., Antoniani, B., Di Benedetto, A., Santoro, R., Germoni, S., De Angelis, F., et al. (2012). miR-10b*, a master inhibitor of the cell cycle, is down-regulated in human breast tumours. EMBO Mol. Med. *4*, 1214–1229.

Bonnomet, A., Syne, L., Brysse, A., Feyereisen, E., Thompson, E.W., Noël, A., Foidart, J.M., Birembaut, P., Polette, M., and Gilles, C. (2012). A dynamic in vivo model of epithelial-to-mesenchymal transitions in circulating tumor cells and metastases of breast cancer. Oncogene *31*, 3741–3753.

Buffa, F.M., Camps, C., Winchester, L., Snell, C.E., Gee, H.E., Sheldon, H., Taylor, M., Harris, A.L., and Ragoussis, J. (2011). microRNA-associated progression pathways and potential therapeutic targets identified by integrated mRNA and microRNA expression profiling in breast cancer. Cancer Res. *71*, 5635–5645.

Cancer Genome Atlas Network (2012). Comprehensive molecular portraits of human breast tumours. Nature *490*, 61–70.

Chi, S.W., Zang, J.B., Mele, A., and Darnell, R.B. (2009). Argonaute HITS-CLIP decodes microRNA-mRNA interaction maps. Nature *460*, 479–486.

DeLuca, D.S., Levin, J.Z., Sivachenko, A., Fennell, T., Nazaire, M.D., Williams, C., Reich, M., Winckler, W., and Getz, G. (2012). RNA-SeQC: RNA-seq metrics for quality control and process optimization. Bioinformatics *28*, 1530–1532.

Enerly, E., Steinfeld, I., Kleivi, K., Leivonen, S.K., Aure, M.R., Russnes, H.G., Rønneberg, J.A., Johnsen, H., Navon, R., Rødland, E., et al. (2011). miRNA-mRNA integrated analysis reveals roles for miRNAs in primary breast tumors. PLoS ONE *6*, e16915.

Fan, J., and Bertino, J.R. (1997). Functional roles of E2F in cell cycle regulation. Oncogene *14*, 1191–1200.

Flicek, P., Ahmed, I., Amode, M.R., Barrell, D., Beal, K., Brent, S., Carvalho-Silva, D., Clapham, P., Coates, G., Fairley, S., et al. (2013). Ensembl 2013. Nucleic Acids Res. *41*, D48–D55.

Frith, M.C., Saunders, N.F., Kobe, B., and Bailey, T.L. (2008). Discovering sequence motifs with arbitrary insertions and deletions. PLoS Comput. Biol. *4*, e1000071.

Granit, R.Z., Gabai, Y., Hadar, T., Karamansha, Y., Liberman, L., Waldhorn, I., Gat-Viks, I., Regev, A., Maly, B., Darash-Yahana, M., et al. (2013). EZH2 promotes a bi-lineage identity in basal-like breast cancer cells. Oncogene *32*, 3886–3895.

Hafner, M., Landthaler, M., Burger, L., Khorshid, M., Hausser, J., Berninger, P., Rothballer, A., Ascano, M., Jr., Jungkamp, A.C., Munschauer, M., et al. (2010). Transcriptome-wide identification of RNA-binding protein and microRNA target sites by PAR-CLIP. Cell *141*, 129–141.

Helwak, A., Kudla, G., Dudnakova, T., and Tollervey, D. (2013). Mapping the human miRNA interactome by CLASH reveals frequent noncanonical binding. Cell *153*, 654–665.

Kallergi, G., Papadaki, M.A., Politaki, E., Mavroudis, D., Georgoulias, V., and Agelaki, S. (2011). Epithelial to mesenchymal transition markers expressed in circulating tumour cells of early and metastatic breast cancer patients. Breast Cancer Res. *13*, R59.

Keene, J.D., Komisarow, J.M., and Friedersdorf, M.B. (2006). RIP-Chip: the isolation and identification of mRNAs, microRNAs and protein components of ribonucleoprotein complexes from cell extracts. Nat. Protoc. *1*, 302–307.

Kishore, S., Jaskiewicz, L., Burger, L., Hausser, J., Khorshid, M., and Zavolan, M. (2011). A quantitative analysis of CLIP methods for identifying binding sites of RNA-binding proteins. Nat. Methods *8*, 559–564.

Lal, A., Navarro, F., Maher, C.A., Maliszewski, L.E., Yan, N., O'Day, E., Chowdhury, D., Dykxhoorn, D.M., Tsai, P., Hofmann, O., et al. (2009). miR-24 Inhibits cell proliferation by targeting E2F2, MYC, and other cell-cycle genes via binding to "seedless" 3'UTR microRNA recognition elements. Mol. Cell *35*, 610–625.

Lal, A., Thomas, M.P., Altschuler, G., Navarro, F., O'Day, E., Li, X.L., Concepcion, C., Han, Y.C., Thiery, J., Rajani, D.K., et al. (2011). Capture of microRNA-bound mRNAs identifies the tumor suppressor miR-34a as a regulator of growth factor signaling. PLoS Genet. *7*, e1002363.

Lamouille, S., Subramanyam, D., Blelloch, R., and Derynck, R. (2013). Regulation of epithelial-mesenchymal and mesenchymal-epithelial transitions by microRNAs. Curr. Opin. Cell Biol. *25*, 200–207.

Li, M., Lee, K.F., Lu, Y., Clarke, I., Shih, D., Eberhart, C., Collins, V.P., Van Meter, T., Picard, D., Zhou, L., et al. (2009). Frequent amplification of a chr19q13.41 microRNA polycistron in aggressive primitive neuroectodermal brain tumors. Cancer Cell *16*, 533–546.

Liu, C., Xu, P., Lamouille, S., Xu, J., and Derynck, R. (2009). TACE-mediated ectodomain shedding of the type I TGF-beta receptor downregulates TGF-beta signaling. Mol. Cell *35*, 26–36.

Loeb, G.B., Khan, A.A., Canner, D., Hiatt, J.B., Shendure, J., Darnell, R.B., Leslie, C.S., and Rudensky, A.Y. (2012). Transcriptome-wide miR-155 binding map reveals widespread noncanonical microRNA targeting. Mol. Cell *48*, 760–770.

Lowery, A.J., Miller, N., Devaney, A., McNeill, R.E., Davoren, P.A., Lemetre, C., Benes, V., Schmidt, S., Blake, J., Ball, G., and Kerin, M.J. (2009). MicroRNA signatures predict oestrogen receptor, progesterone receptor and HER2/neu receptor status in breast cancer. Breast Cancer Res. *11*, R27.

Lv, Q., Wang, W., Xue, J., Hua, F., Mu, R., Lin, H., Yan, J., Lv, X., Chen, X., and Hu, Z.W. (2012). DEDD interacts with PI3KC3 to activate autophagy and attenuate epithelial-mesenchymal transition in human breast cancer. Cancer Res. *72*, 3238–3250.

Ma, L., Young, J., Prabhala, H., Pan, E., Mestdagh, P., Muth, D., Teruya-Feldstein, J., Reinhardt, F., Onder, T.T., Valastyan, S., et al. (2010). miR-9, a MYC/MYCN-activated microRNA, regulates E-cadherin and cancer metastasis. Nat. Cell Biol. *12*, 247–256.

Martin, M. (2011). Cutadapt removes adapter sequences from high-throughput sequencing reads. EMBnet.journal *17*, 3.

Matys, V., Kel-Margoulis, O.V., Fricke, E., Liebich, I., Land, S., Barre-Dirrie, A., Reuter, I., Chekmenev, D., Krull, M., Hornischer, K., et al. (2006). TRANSFAC and its module TRANSCompel: transcriptional gene regulation in eukaryotes. Nucleic Acids Res. *34*, D108–D110.

Milewski, R.C., Chi, N.C., Li, J., Brown, C., Lu, M.M., and Epstein, J.A. (2004). Identification of minimal enhancer elements sufficient for Pax3 expression in neural crest and implication of Tead2 as a regulator of Pax3. Development *131*, 829–837.

Ørom, U.A., Nielsen, F.C., and Lund, A.H. (2008). MicroRNA-10a binds the 5'UTR of ribosomal protein mRNAs and enhances their translation. Mol. Cell *30*, 460–471.

Rippe, V., Dittberner, L., Lorenz, V.N., Drieschner, N., Nimzyk, R., Sendt, W., Junker, K., Belge, G., and Bullerdiek, J. (2010). The two stem cell microRNA gene clusters C19MC and miR-371-3 are activated by specific chromosomal rearrangements in a subgroup of thyroid adenomas. PLoS ONE *5*, e9485.

Sieuwerts, A.M., Mostert, B., Bolt-de Vries, J., Peeters, D., de Jongh, F.E., Stouthard, J.M., Dirix, L.Y., van Dam, P.A., Van Galen, A., de Weerd, V., et al. (2011). mRNA and microRNA expression profiles in circulating tumor cells and primary tumors of metastatic breast cancer patients. Clin. Cancer Res. *17*, 3600–3618.

Song, Y., Washington, M.K., and Crawford, H.C. (2010). Loss of FOXA1/2 is essential for the epithelial-to-mesenchymal transition in pancreatic cancer. Cancer Res. *70*, 2115–2125.

Song, S.J., Poliseno, L., Song, M.S., Ala, U., Webster, K., Ng, C., Beringer, G., Brikbak, N.J., Yuan, X., Cantley, L.C., et al. (2013). MicroRNA-antagonism regulates breast cancer stemness and metastasis via TET-family-dependent chromatin remodeling. Cell *154*, 311–324.

Su, H., Trombly, M.I., Chen, J., and Wang, X. (2009). Essential and overlapping functions for mammalian Argonautes in microRNA silencing. Genes Dev. *23*, 304–317.

Tan, S.M., Altschuler, G., Zhao, T.Y., Ang, H.S., Yang, H., Lim, B., Vardy, L., Hide, W., Thomson, A.M., and Lareu, R.R. (2014). Divergent LIN28-mRNA associations result in translational suppression upon the initiation of differentiation. Nucleic Acids Res. *42*, 7997–8007.

Tay, Y., Zhang, J., Thomson, A.M., Lim, B., and Rigoutsos, I. (2008). MicroRNAs to Nanog, Oct4 and Sox2 coding regions modulate embryonic stem cell differentiation. Nature *455*, 1124–1128.

Thomas, M., Lieberman, J., and Lal, A. (2010). Desperately seeking microRNA targets. Nat. Struct. Mol. Biol. *17*, 1169–1174.

Trapnell, C., Pachter, L., and Salzberg, S.L. (2009). TopHat: discovering splice junctions with RNA-Seq. Bioinformatics *25*, 1105–1111.

Venkov, C., Plieth, D., Ni, T., Karmaker, A., Bian, A., George, A.L., Jr., and Neilson, E.G. (2011). Transcriptional networks in epithelial-mesenchymal transition. PLoS One *6*, e25354.

Vetter, G., Saumet, A., Moes, M., Vallar, L., Le Béchec, A., Laurini, C., Sabbah, M., Arar, K., Theillet, C., Lecellier, C.H., and Friederich, E. (2010). miR-661 expression in SNAI1-induced epithelial to mesenchymal transition contributes to breast cancer cell invasion by targeting Nectin-1 and StarD10 messengers. Oncogene *29*, 4436–4448.

Wang, L., Wang, S., and Li, W. (2012). RSeQC: quality control of RNA-seq experiments. Bioinformatics *28*, 2184–2185.

Wiggan, O., Fadel, M.P., and Hamel, P.A. (2002). Pax3 induces cell aggregation and regulates phenotypic mesenchymal-epithelial interconversion. J. Cell Sci. *115*, 517–529.

Wu, S., Huang, S., Ding, J., Zhao, Y., Liang, L., Liu, T., Zhan, R., and He, X. (2010). Multiple microRNAs modulate p21Cip1/Waf1 expression by directly targeting its 3′ untranslated region. Oncogene *29*, 2302–2308.

Xia, Z., Clark, P., Huynh, T., Loher, P., Zhao, Y., Chen, H.W., Ren, P., Rigoutsos, I., and Zhou, R. (2012). Molecular dynamics simulations of Ago silencing complexes reveal a large repertoire of admissible 'seed-less' targets. Sci. Rep. *2*, 569.

Yang, J., and Weinberg, R.A. (2008). Epithelial-mesenchymal transition: at the crossroads of development and tumor metastasis. Dev. Cell *14*, 818–829.

Zisoulis, D.G., Lovci, M.T., Wilbert, M.L., Hutt, K.R., Liang, T.Y., Pasquinelli, A.E., and Yeo, G.W. (2010). Comprehensive discovery of endogenous Argonaute binding sites in Caenorhabditis elegans. Nat. Struct. Mol. Biol. *17*, 173–179.